Journal of Materials Chemistry C

PAPER

Benzoselenadiazole and benzotriazole directed electrophilic C-H borylation of conjugated donor-acceptor materials†

Received 00th January 20xx,
Accepted 00th January 20xx

DOI: 10.1039/x0xx00000x

www.rsc.org/

Barada P. Dash,[a,d] Iain Hamilton,[b] Daniel J. Tate,[a] Daniel L. Crossley,[c] Ji-Seon Kim,[b] Michael J. Ingleson*[c] and Michael L. Turner*[a,c]

Benzoselenadiazole and benzotriazole directed electrophilic borylation using BCl_3 results in the C-H functionalization of an adjacent aromatic unit and produces fused boracycles. Subsequent arylation at boron afforded stable products displaying large bathochromic shifts and significantly reduced LUMO energy levels. OLEDs fabricated containing borylated benzoselenadiazole derivatives showed emission centered at 723 nm in the near infra-red region of the spectrum.

Introduction

Control of the frontier molecular orbital energies of conjugated molecules is essential to optimize the materials for use in a range of organic electronic devices. By combining electron-rich donor and electron-poor acceptor units in a conjugated material a significant reduction in the HOMO-LUMO energy separation can be achieved.[1,2] However, precise tuning of the HOMO and LUMO energies has generally involved multi-step synthetic manipulation of the molecular framework of the donor and acceptor units. A simpler approach is via modification of pre-formed donor-acceptor materials as exemplified in recent work where fluorine substituents on a benzothiadiazole unit of a conjugated polymer undergo nucleophilic aromatic substitution with oxygen and sulfur nucleophiles. This post-polymerisation modification introduces a wide range of functional groups on the polymers.[3] A related simple approach that decreases the LUMO energy involves coordination of Lewis acids (e.g. BX_3, X = halide) to the acceptor units (e.g. benzothiadiazole, BT). Adduct formation with BX_3 leads to a considerable decrease in both the energy of the LUMO and the band gap.[4] The principal drawback of the Lewis acid binding strategy is that the Lewis adducts are sensitive to moisture and Lewis bases as these cleave the dative bond between the acceptor and the Lewis acid.

The stability of coordinated Lewis acidic boranes can be enhanced by concurrent formation of the dative bond and a new covalent C-B bond to form a boracycle containing the chelated Lewis acid adduct.[5,6] A number of efficient synthetic methods have been reported for boracycle formation particularly using directed (by a Lewis basic moiety) electrophilic C-H borylation of aromatics and hetero aromatics.[7] This approach has been applied by some of us to the borylative fusion of D-A conjugated materials (both polymers and small molecules) containing the BT acceptor (e.g. **A**, Scheme 1). The resulting borylated materials contain BT units fused to a variety of donors including fluorene, thiophene and phenyl units (*e.g.* **B** and **C**). These materials are stable to ambient moisture and are highly emissive with a low band gap (< 2 eV).[7b,7e, 7h]

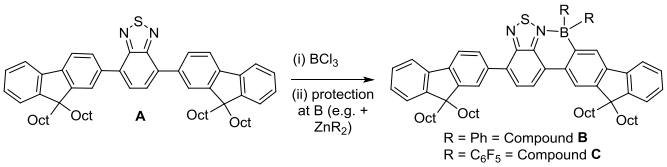

Scheme 1: Electrophilic borylation and subsequent protection of a benzothiadiazole D-A-D compound (**A**)

Donor acceptor conjugated materials based on the related acceptor units benzoselenadiazole (BSe)[8-10] and benzotriazole (BTz)[11-14] have been reported, and D-A materials containing these units also contain a N-directing group appropriate for electrophilic C-H borylation. However, to the best of our knowledge these acceptors have not previously been used in directed electrophilic C-H borylation.

Herein, we report the BSe and BTz directed C-H borylation of donor acceptor systems **4** and **5** as shown in Scheme 2. These reactions lead to a dramatic decrease in the energy of the LUMO and large red shifts in the absorption and emission spectra of the compounds **8-11**. The benzoselenadiazole

[a] Organic Materials Innovation Centre, School of Chemistry, University of Manchester, Manchester M13 9PL, United Kingdom. E-mail: Michael.turner@manchester.ac.uk
[b] Department of Physics and Centre for Plastic Electronics, Imperial College London, London, SW7 2AZ, UK
[c] School of Chemistry, University of Manchester, Manchester M13 9PL, United Kingdom. E-mail: Michael.ingleson@manchester.ac.uk
[d] Department of Chemistry, Siksha 'O' Anusandhan University, Bhubaneswar, Odisha 751 030, India

† Electronic Supplementary Information (ESI) available: Experimental details and characterization data for all new compounds, thin film UV and fluorescence data, molecular orbital energy level diagram of benzotriazole compounds and theoretical HOMO-LUMO energy data. See DOI: 10.1039/x0xx00000x

derivatives, **8,9**, were found to have smaller band gaps and emission further into the far red region of the spectrum than the previously reported benzothiadiazole analogues (**B**, **C**).

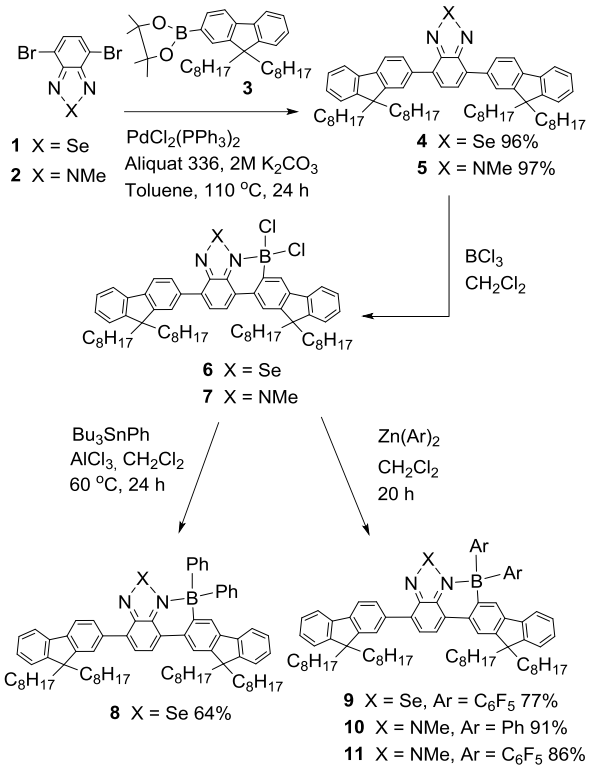

Scheme 2 Synthesis and borylation of fluorene-BTz and BSe D-A-D compounds

Results and Discussion

Bis(9,9-dioctylfluorene) benzoselenadiazole (F8-BSe-F8, **4**) and bis(9,9-dioctylfluorene) benzotriazole (F8-BTz-F8, **5**, Scheme 2) were readily synthesised via the Suzuki-Miyaura cross coupling of the respective dibromides (**1** and **2**) with the boronic acid pinacol ester **3** in excellent yields.[14] The addition of BCl_3 to DCM solutions of **4** and **5** resulted in coordination of boron to the nitrogen sites on BSe and BTz and electrophilic C–H borylation to form the fused boracyclic intermediates **6** and **7**, respectively (Scheme 2). Borylation was quantitative (by in-situ ^{1}H NMR spectroscopy, see SI) in an open system with HCl released as a gaseous by-product. As reported earlier for the BT derivatives,[7b] borylation occurred exclusively at the less sterically hindered C_3 position and no borylation was observed at the more hindered C_1 position. Arylation at boron for compound **6** was accomplished by treatment with tributylphenylstannane in the presence of catalytic $AlCl_3$ to form **8**,[7c] arylation of compounds **6** and **7** was accomplished by using diarylzinc reagents to form **9**, **10** and **11**. All borylated products were formed in good yields.

The photophysical properties of **8**, **9**, **10** and **11** were investigated by solution UV/Vis absorption and photoluminescence (PL) spectroscopy in toluene (Figure 1 and Table 1). As expected, borylation led to significant red shifts in the absorption and emission spectrum of these compounds. Relative to the unborylated fluorene-substituted BSe analogue **4**, compounds **8** and **9** showed a red-shifted absorbance (148 and 170 nm, respectively) and red shifted emission (174 and 211 nm, respectively). Both shifts in the absorbance and emission maxima of BSe derivatives were found to be higher than the shifts observed for the reported borylated BT derivatives **A**, **B** and **C**.[7b]

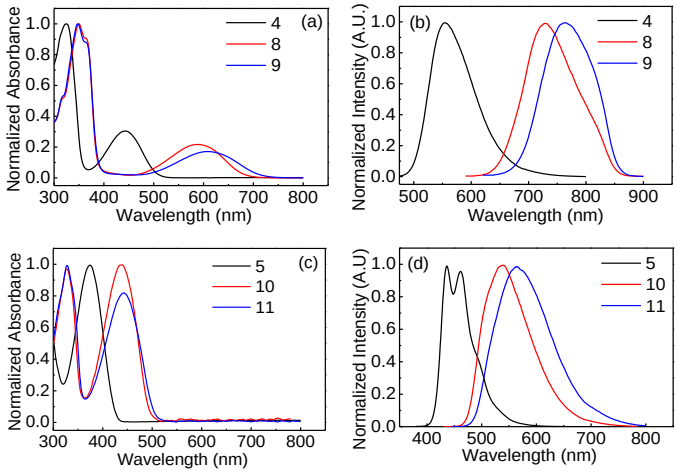

Fig. 1 (a) Normalized absorption and (b) normalized fluorescence spectra of fluorene-benzoselenadiazole D-A-D compounds. (c) Normalized absorption and (d) normalized fluorescence spectra of fluorene-benzotriazole D-A-D compounds. UV and Fluorescence spectra were measured by exciting their solutions in toluene at their absorption maxima (1 x 10^{-5} M concentration).

Table 1 Summary of solution UV and fluorescence data

	$\lambda_{max\text{-}abs}$ [a] (nm)	$\lambda_{max\text{-}em}$ [a] (nm)	Stokes shift (cm^{-1})	Optical band gap [b] (eV)	Quantum Yield (Φ) [c] (%)
4	442	554	4570	2.44	37
8	590	728	3210	1.82	4
9	612	765	3270	1.64	0.4
5	374	462	5090	2.91	79
10	437	539	4330	2.51	58
11	443	564	4840	2.45	43
A [d]	419	540	5350	2.59	-
B [d]	559	702	3640	1.92	10
C [d]	579	730	3570	1.83	2

[a]In toluene 1x10^{-5} M. [b]Band gap estimated from onset of absorption. [c]Φ was calculated against quinine sulfate, cresyl violet and fluorescein as standards.[15] [d] from ref 7b

Compounds **8** and **9** showed emission maxima at 728 nm and 765 nm, respectively in toluene, and their emission continued significantly into the near-infrared spectral region. These emission maxima are at higher wavelengths than observed for the BT analogues,[7b] consistent with the smaller band gap for BSe Vs BT D-A compounds (e.g. compare compounds **4** and **A** in Table 1). BTz derivatives showed red shifts on borylation to a lesser extent relative to the BSe and the BT derivatives. In the series of borylated compounds the highest reduction in band gap was observed for the BSe derivatives, the lowest for

the BTz derivatives and intermediate for the BT derivatives. It was observed that the exocyclic boron substituent C_6F_5 had a more pronounced effect on the photophysical properties. The solution quantum yields obtained in toluene for borylated products **8**, **9**, **10** and **11** were found to be lower than their unborylated precursors with highest reduction in the quantum yield observed for the borylated BSe derivatives consistent with the energy gap law, with the low band gap in the BSe borylated compounds accelerating non-radiative processes.

Thin film UV and fluorescence spectra of BSe derivatives showed larger red shifts in their absorption and emission maxima compared to the data obtained in solution (See SI). Borylated BSe derivatives **8** and **9** showed thin film absorbance maxima at 592 nm and 624 nm, respectively, and emission maxima at 763 nm and 820 nm, respectively. The emission continues well into the near-infrared spectral region. On the contrary, the borylated BTz derivatives did not show such enhanced red shifts in their thin film absorbance and emission maxima compared to the values obtained in solution (See SI). BTz derivatives **10** and **11** showed thin film absorbance maxima at 439 nm and 449 nm, respectively and emission maxima at 547 nm and 569 nm respectively.

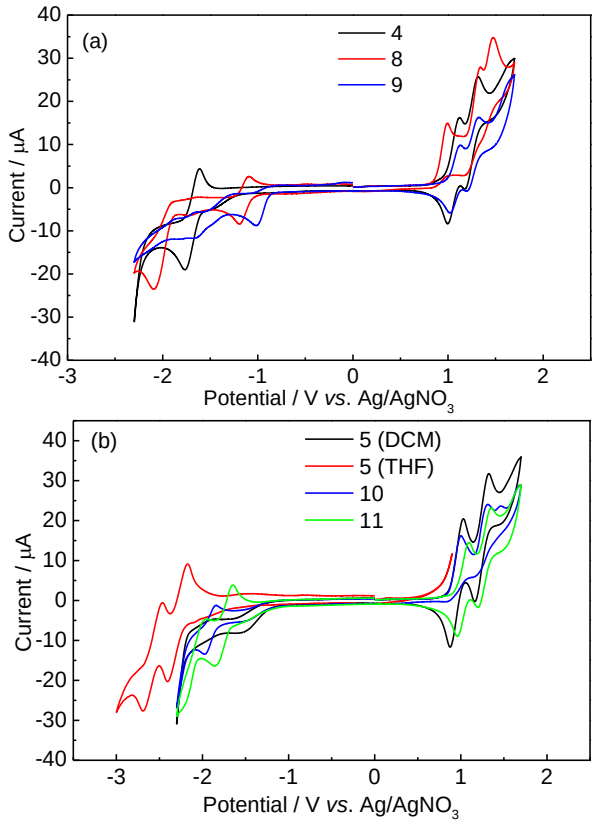

Fig. 2. Cyclic voltammagrams of (a) F8-BSe D-A-D compounds (b) F8-BTz D-A-D compounds measured in DCM (1 mM) with $[^nBu_4N][PF_6]$ (0.1 M) as the supporting electrolyte at a scan rate of 100 mV/s relative to Fc/Fc^+ redox couple standard. Compound **5** was also run in THF.

Cyclic voltammetry gave further insight into the effect of variation in the acceptor on the frontier molecular orbital energies (Figure 2 and Table 2). All compounds were stable to the electrolyte $[nBu_4N][PF_6]$ used for the experiments. In general, the onset of reduction processes for borylated products are found to be significantly less negative whereas the onset of oxidation processes are less affected as previously observed.[7b]

Table 2. Summary of cyclic voltammetry data

Comp.	E_{ox}^{onset} (V)	E_{red}^{onset} (V)	HOMO[a] (eV)	LUMO[a] (eV)	Band gap (eV)
4	0.96	-1.56	-6.35	-3.83	2.52
8	0.87	-1.03	-6.26	-4.36	1.9
9	0.99	-0.87	-6.38	-4.52	1.86
5	0.87	-2.21	-6.26	-3.18	3.08
10	0.86	-1.81	-6.25	-3.58	2.67
11	0.94	-1.71	-6.33	-3.68	2.65
A[b]	0.88	-1.87	-6.27	-3.52	2.75
B[b]	0.80	-1.28	-6.19	-4.11	2.08
C[b]	0.85	-1.12	-6.24	-4.27	1.97

[a]Potentials are given relative to Fc/Fc^+ redox couple which is taken to be 5.39 eV below vacuum.[16] [b] From ref. 6b

Thus borylative fusion has minimal effect on the HOMO energy but results in a significant reduction in the LUMO energy leading to a considerable band gap reduction. For the BTz derivative **5** cyclic voltammetry was carried out in two different solvents, THF was used for the reduction processes and DCM was for the oxidation processes. BSe derivatives **4**, **8** and **9** showed a single fully reversible reduction process, multiple reversible oxidation peaks in dichloromethane and have the lowest LUMO energy in each case from the series of BSe, BT and BTz. The strongly electron withdrawing exocyclic boron substituent C_6F_5 groups have the most dramatic effect on the lowering of LUMO. The maximum reduction in the LUMO level was observed for BSe derivative **9** (0.69 eV) and moderate reduction in the LUMO level was observed for the triazole derivatives with BT in between. Although the HOMO energy levels of BTz derivatives are comparable with the BT and BSe derivatives, the LUMO energy levels are higher leading to the larger electrochemical band gap observed for BTz derivatives. Not only does the BSe congener have the lowest LUMO energy before borylation of this series (consistent with other BT Vs BSe D-A materials),[17] it is also more affected by borylation, resulting in the overall considerable decrease in band gap on borylation.

The lowering of the band gap via borylation has been further assessed via DFT calculations at the B3LYP/6-31G(d,p) level with CPCM solvation (dichloromethane), with the octyl chains replaced with methyl (See Figures S1 to S3, SI). The trends in calculated energies were consistent with the relative energies of frontier orbitals from CV studies (Figure 3).

To explore the potential application of these compounds as emissive materials, a series of OLED devices were fabricated via solution processing using compounds **8**, **10** and **11** as emitters. To achieve superior film quality and minimise aggregation induced quenching, the emitters were dispersed in a host matrix with a 5wt% loading ratio. For compound **8**,

poly(9,9'-dioctyl-fluorene-alt-benzothiadiazole (F8BT) was chosen as host due to the good spectral overlap of F8BT PL emission with the absorption peak of **8** (Figure S5(a)). For compounds **10** and **11**, poly(9,9-dioctyl fluorene) (PFO) was used as the higher energy emission of PFO overlaps well with the higher energy absorption of BTz derivatives (Figure S5(b)). Photoluminescence measurements of compounds **8**, **10** and **11** at 5% loading in their respective hosts (Figure S5 (c) and (d)) confirm good energy transfer between host and guest.

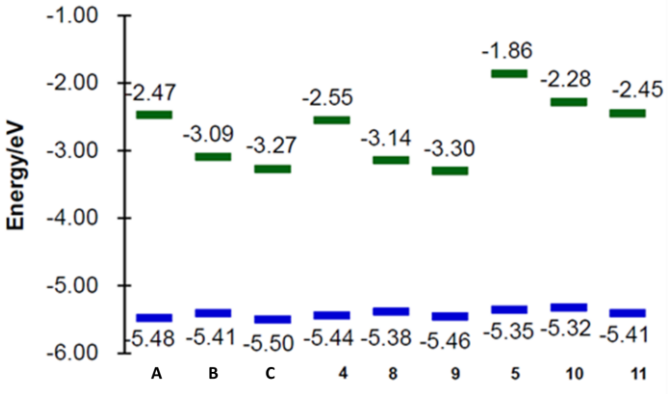

Fig. 3. The HOMO and LUMO energy level diagram of fluorene-benzothiadiazole, fluorene-benzoselenadiazole and fluorene-benzotriazole containing D-A-D compounds. Full geometry optimization and HOMO-LUMO energy were obtained by using B3LYP/6-31G(d,p) level CPCM solvation (dichloromethane).The octyl group has been replaced with methyl throughout.

For all devices, an interlayer of poly[(9,9-dioctylfluorenyl-2,7-diyl)-co-(4,4'-(N-(4-sec-butylphenyl)-diphenylamine))] (TFB) was utilized. TFB has previously been shown to improve OLED device efficiency by preventing quenching of excitons formed in the emissive layer due to the wide energy gap of the TFB (>3.0 eV) blocking exciton migration, as well as acting as a good hole transporting layer due to its low ionization potential (5.33 eV) and high hole mobility.[18,19] A thermally evaporated small-molecule electron transport layer was not used in these devices to reduce device complexity, thus showing efficient OLED device can be fabricated using solution-processing methods. The device structure used was thus ITO/PEDOT:PSS/TFB/Emission Layer/Ca/Al. An energy level diagram of the devices is shown in Figure S6 (see SI). Figure 4 and Table 3 show the best performing device characteristics for 95 wt% F8BT: 5 wt% **8** (device 1), 95 wt% PFO: 5 wt% **10** (device 2) and 95 wt% PFO: 5 wt% **11** (device 3) emission layer (EML) OLEDs. The average performance of each device is shown in Table S3 (see SI). Due to the small band gap of compound **8**, the electroluminescence (EL) spectra of device 1 shows a broad emission peak at λ_{max} = 723 nm extending into the near infra-red (NIR), with minimal host emission. The device displays a turn-on voltage of 4.3 V and a maximum EQE of 0.12%. The maximum EQE of NIR OLEDs containing the BSe derivative **8 (BPh_2)** is comparable to contemporary solution processed NIR OLED[20] and light emitting electrochemical cell (LEC) devices.[21]

The wider band gap of compounds **10** and **11** mean that devices 2 and 3 emit in the visible region. Device 2 exhibits an emission peak at λ_{max} = 540 nm, whilst device 3 shows a slightly broader maximum emission peak at λ_{max} = 568 nm. Both devices show minimal host emission, whilst their EL emission is slightly blue-shifted compared to their respective PL spectra. The devices emit brightly, with a maximum luminance of L_{max} = 1424 cd/m² for device 2 and L_{max} = 906 cd/m² for device 3. The maximum luminous and luminous power efficiencies for device 2 are 0.36 cd/A and 0.22 lm/W

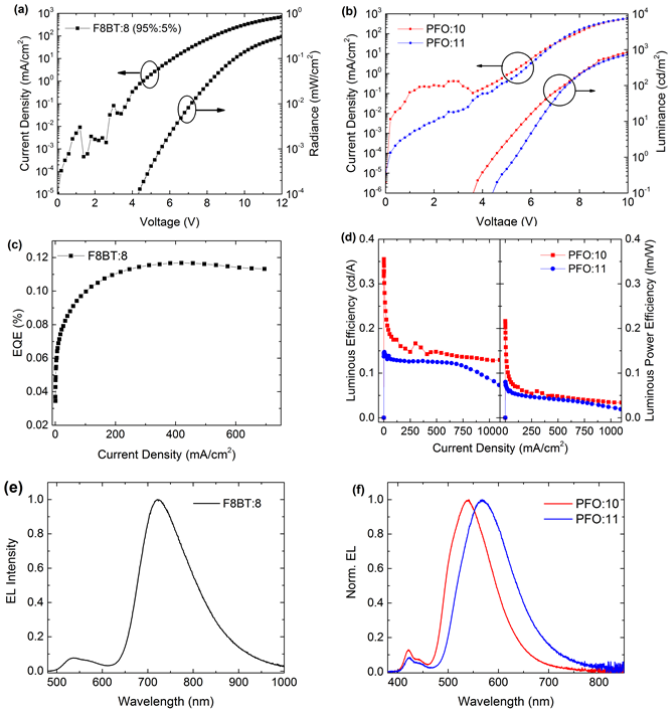

respectively, whilst device 3 shows maximum efficiencies of 0.15 cd/A and 0.08 lm/W. The difference in efficiencies could be accounted for by the lower PLQY of compound **10** compared to compound **11**.

Fig 4. OLED characteristics for device 1 (black), device 2 (red) and device 3 (blue). J-V-R, EQE and EL spectra data for device 1 is plotted in (a), (c) and (e) whilst J-V-L, luminous (cd/A) and luminous power (lm/W) and EL spectra for devices 2 and 3 are plotted in (b), (d) and (f).

Table 3. Summary of best performing OLED device parameters

Device	Comp.	V_{on}[a] (V)	EL λ_{max}[b] (nm)	Max. EQE[c] (%)	Max η^d (cd/A)	Max η_w[e] (lm/W)
1	**8**	4.3	723	0.12	-	-
2	**10**	3.8	540	0.10	0.36	0.22
3	**11**	4.6	568	0.05	0.15	0.08

[a] Turn-on voltage. [b] Wavelength at which electroluminescence spectra is at maximum. [c] Maximum external quantum efficiency. [d] Maximum luminous efficiency. [e] Maximum luminous power efficiency

Conclusions

In summary, we have reported a simple approach for benzoselenadiazole (BSe) and benzotriazole (BTz) directed borylative fusion of donor-acceptor materials. *In situ* arylation of boron using either organotin or diarylzinc reagents resulted in the formation of air and moisture stable boracycles that display large bathochromic shifts in absorption and emission spectra in solution and as thin films. Among the compounds, BSe derivative **9** showed a red shift in absorbance and emission by 170 nm and 211 nm, respectively. Furthermore, the borylated BSe derivatives emitted in the near-infrared spectral region in solution and thin films. These studies indicate that the borylative fusion of BSe and BTz containing donor-acceptor oligomers is an attractive method for generating materials with low lying LUMOs, with BSe derivatives having smaller band gaps than the previously reported benzothiadiazole derivatives. Currently, this borylation strategy is being extended to polymeric D-A materials.

Experimental section

Synthesis of 4

4,7-dibromobenzo[c][1,2,5] selenadiazole **1** (350 mg, 1.19 mmol), 9,9-Di-n-octylfluorene-2-boronic acid pinacol ester **3** (1.66 g, 3.21 mmol) and $PdCl_2(PPh_3)_2$ (70.2 mg, 0.12 mmol, 10 mol%) were mixed in anhydrous toluene (20 mL) under an nitrogen atmosphere. Then 2M K_2CO_3 (3 mL) and Aliquat 336 (0.2 mL) were added to it and stirred for 22 h at 110 °C under reflux. The mixture was cooled to room temperature and then water 30 mL was added to it and then extracted thrice with ethyl acetate. The organic portion was washed with brine and dried over $MgSO_4$. After evaporating the solvent, the residue was purified by column chromatography on silica gel [eluent: 0.5%-1% ethyl acetate in petroleum ether] to afford **4** as a yellow solid. Yield: 1.1 g, 96%. ^{1}H NMR (400MHz, $CDCl_3$): δ 8.01 (d, 2H, J = 8 Hz), 7.89 (d, 4H, J = 8 Hz), 7.80 (d, 2H, J = 4), 7.76 (s, 2H), 7.43-7.35 (m, 6H), 2.13-2.00 (m, 8H), 1.24-1.13 (m, 48H), 0.84 (t, 12H, J = 6 Hz). ^{13}C NMR (100MHz, $CDCl_3$): δ 160.0, 151.3, 151.0, 141.2, 140.7, 136.9, 135.4, 128.5, 128.3, 127.2, 126.9, 124.1, 123.0, 119.9, 119.5, 55.2, 40.3, 31.9, 30.1, 29.2, 23.9, 22.6, 14.1. HRMS (m/z) calc. for $C_{64}H_{84}N_2Se$: 961.5878, found 961.5844 $[M+H]^+$.

Compound 5

4,7-dibromo-2-methyl-2H-benzo[d][1,2,3]triazole **2** (350 mg, 1.2 mmol), 9,9-Di-n-octylfluorene-2-boronic acid pinacol ester **3** (1.68 g, 3.25 mmol) and $PdCl_2(PPh_3)_2$ (70.2 mg, 0.12 mmol, 10 mol%) were mixed in dry toluene (20 mL) under an nitrogen atmosphere. Then 2M K_2CO_3 (3 mL) and Aliquat 336 (0.2 mL) were added to it and stirred for 22 h at 110 °C under reflux. The mixture was cooled to room temperature and then water 30 mL was added to it and then extracted thrice with ethyl acetate. The organic portion was washed with brine and dried over $MgSO_4$. After evaporating the solvent, the residue was purified by column chromatography on silica gel [eluent: 0.2%-1% ethyl acetate in petroleum ether] to afford **5** as a pale green solid. Yield: 1.06 g, 97%. ^{1}H NMR (400 MHz, $CDCl_3$): δ 8.07 (d, 1H, J = 4 Hz), 8.06 (d, 1H, J = 4 Hz), 7.91 (s, 2H), 7.77 (d, 2H, J = 8 Hz), 7.69 (s, 1H), 7.67 (s, 1H), 7.65 (s, 1H), 7.31-7.22 (m, 6H), 4.53 (s, 3H), 2.03-1.89 (m, 8H), 1.12-0.99 (m, 48H), 0.72 (t, 12H, J = 6 Hz). ^{13}C NMR (100 MHz, $CDCl_3$): δ 151.3, 151.2, 144.0, 141.0, 140.8, 136.2, 130.6, 127.6, 127.1, 126.8, 124.6, 123.0, 122.9, 119.9, 119.8. HRMS (m/z) calc. for $C_{65}H_{87}N_3$: 910.6978, found 910.6988 $[M+H]^+$.

Compound 6

BCl_3 (1M solution in dichloromethane) (0.83 mL, 0.83 mmol) was added to a yellow solution of **4** (200 mg, 0.21 mmol) in anhydrous dichloromethane (10 mL) in a Schlenk flask resulting in a colour change to dark blue and the reaction mixture was stirred overnight under the dynamic flow of nitrogen. The solvent and excess BCl_3 was removed under reduced pressure and compound **6** was isolated as a dark blue solid. The compound was further used without any purification. ^{1}H NMR (400 MHz, CD_2Cl_2): δ 8.50 (d, 1H, J = 8 Hz), 8.45 (s, 1H), 8.00 (s, 1H), 7.96 (d, 1H, J = 4 Hz), 7.91 (s, 2H), 7.90-7.87 (m, 2H), 7.83-7.81 (m, 1H),7.44-7.37 (m, 6H), 2.09-2.04 (m, 8H), 1.24-1.07 (m, 48H), 0.86-0.83 (m, 12H). ^{13}C NMR (100MHz, CD_2Cl_2): δ 159.1, 151.4, 151.3, 151.2, 151.2, 149.9, 143.2, 142.5, 140.4, 140.2, 135.4, 133.9, 130.7, 128.5, 128.3, 127.9, 127.8, 127.7, 127.0, 127.0, 125.3. 124.2, 123.1, 122.8, 120.9, 120.2, 119.9, 116.1, 55.5, 55.1, 53.4, 40.7, 40.3, 31.8, 31.8, 30.1, 30.0, 29.3, 29.2, 29.2, 23.9, 23.9, 22.6, 22.6, 14.1, 14.0. ^{11}B NMR (proton decoupled, 128.4 MHz): 2.23 (Broad).

Compound 7

BCl_3 (1 M solution in dichloromethane) (0.87 mL, 0.88 mmol) was added to a pale green solution of **5** (200 mg, 0.22 mmol) in anhydrous dichloromethane (10 mL) in a Schlenk flask resulting in a colour change to dark blue and the reaction mixture was stirred overnight under the dynamic flow of nitrogen. The solvent and excess BCl_3 was removed under reduced pressure and compound **7** was isolated as a yellow solid. The compound was further used without any purification. ^{1}H NMR (400 MHz, CD_2Cl_2): δ 8.45 (s, 1H), 8.39 (d, 1H, J = 8 Hz), 8.16-8.13 (m, 2H), 8.07-8.05 (m, 2H), 7.97-7.93 (m, 2H), 7.87-7.85 (m, 1H), 7.49-7.41 (m, 6H), 5.25 (s, 3H), 2.18-2.11 (m, 8H), 1.25-1.14 (m, 48H), 0.86-0.83 (m, 12H). ^{13}C NMR (100 MHz, CD_2Cl_2): δ 151.6, 151.4, 151.2, 151.1, 142.8, 142.3, 140.5, 140.3, 134.8, 133.6, 130.9, 128.0, 127.7, 127.6, 127.5, 127.3, 126.9, 125.8, 124.2, 124.1, 123.1, 122.9, 120.1, 115.7, 55.3, 55.1, 44.7, 31.8, 31.7, 30.1, 30.0, 29.3, 29.2, 24.0, 23.9, 22.6, 13.8. ^{11}B NMR (proton decoupled, 128.4 MHz): 7.44 (Broad).

Compound 8

BCl_3 (1M solution in dichloromethane) (0.83 mL, 0.83 mmol) was added to a yellow solution of **4** (200mg, 0.21 mmol) in anhydrous dichloromethane (10 mL) in a Schlenk flask resulting in a colour change to dark blue and the reaction mixture was stirred overnight under the dynamic flow of nitrogen. The solvent and excess BCl_3 was removed under reduced pressure. The resulting blue solid was redissolved in

anhydrous dichloromethane (10 mL) and then $AlCl_3$ (3 mg, 0.021 mmol, 10 mol%) and tributylphenylstannane (0.28 mL, 0.83 mmol) were added to it. It was then stirred in the closed Schlenk flask at 60 °C for 24 h. The mixture was cooled to room temperature and then water 30 mL was added to it and then extracted thrice with dichloromethane. The organic portion was washed with brine and dried over $MgSO_4$. After evaporating the solvent, the residue was purified by column chromatography on base treated (5% Et_3N) silica gel [eluent: 0.5% ethyl acetate, 1% triethylamine in petroleum ether] to afford **8** as a blue solid. Yield: 150 mg, 64%. ^{1}H NMR (400MHz, $CDCl_3$) : δ 8.24 (d, 1H, J = 8 Hz), 7.94 (s, 1H), 7.81-7.75 (m, 5H), 8.70-7.68 (m, 1H), 7.56-7.54 (m, 1H), 7.31-7.22 (m, 7H), 7.20-7.09 (m, 9H), 1.96-1.92 (m, 8H), 1.12-0.98 (m, 48H), 0.72 (t, 12H, J = 6 Hz). ^{13}C NMR (100MHz, $CDCl_3$): δ 159.6, 156.6, 152.9, 151.4, 151.3, 151.2, 148.9, 141.7, 141.0, 140.4, 134.9, 134.6, 134.2, 133.5, 130.8, 130.1, 130.0, 128.2, 127.6, 127.5, 127.1, 126.9, 126.8, 126.7, 126.0, 125.5, 124.0, 124.0, 123.0, 122.8, 120.5, 120.0, 119.8, 116.4, 55.3, 54.8, 46.2, 40.7, 40.3, 31.8, 30.2, 30.1, 29.3, 24.0, 23.9, 22.6, 14.1. ^{11}B NMR (proton decoupled, 128.4 MHz): 3.05 (Broad). HRMS (m/z) calc. for $C_{76}H_{93}BN_2Se$: 1125.6575, found 1125.6684 $[M+H]^+$.

Compound 9

BCl_3 (1 M solution in dichloromethane) (0.83 mL, 0.83 mmol) was added to a yellow solution of **4** (200mg, 0.21 mmol) in anhydrous dichloromethane (10 mL) in a Schlenk flask resulting in a colour change to dark blue and the reaction mixture was stirred overnight under the dynamic flow of nitrogen. The solvent and excess BCl_3 was removed under reduced pressure. The resulting blue solid was redissolved in anhydrous dichloromethane (10 mL) and then $Zn(C_6F_5)_2$ (333 mg, 0.83 mmol) was added to it. It was then stirred in the closed Schlenk flask overnight at room temperature. Then water 30 mL was added to it and then extracted thrice with dichloromethane. The organic portion was washed with brine and dried over $MgSO_4$. After evaporating the solvent, the residue was purified by column chromatography on base treated (5% Et_3N) silica gel [eluent: 0.5% ethyl acetate in petroleum ether] to afford **9** as a blue solid. Yield: 210mg, 77%. ^{1}H NMR (400 MHz, $CDCl_3$): δ 8.35 (d, 1H, J = 8 Hz), 7.94 (s, 1H), 7.82 (d, 1H, J = 8 Hz), 7.76 (d, 3H, J = 4 Hz), 7.69 (d, 1H, J = 4 Hz), 7.65 (s, 1H), 7.60-7.58 (m, 1H), 7.32-7.22 (m, 6H), 1.99-1.92 (m, 8H), 1.14-0.95 (m, 48H), 0.74-0.70 (m, 12H). ^{13}C NMR (100MHz, $CDCl_3$):δ 159.3, 152.7, 151.3, 150.1, 142.6, 140.4, 140.3, 134.7, 134.3, 130.9, 129.0, 128.4, 128.3, 127.7, 127.6, 127.0, 126.8, 126.2, 124.1, 123.0, 122.9, 120.3, 120.1, 119.9, 116.3, 55.3, 54.9, 46.1, 40.7, 40.3, 31.8, 30.1, 29.3, 29.2, 29.1, 23.9, 23.8, 23.7, 22.6, 22.6, 14.1. ^{19}F NMR (376.4 MHz, $CDCl_3$): -131.50 (dd, J = 22.56, 7.52 Hz), -156.87 (t, J = 20.68 Hz), -162.59-162.71 (m). ^{11}B NMR (proton decoupled, 128.4 MHz): 1.48 (Broad). HRMS (m/z) calc. for $C_{76}H_{83}BF_{10}N_2Se$: 1305.5733, found 1305.5714$[M+H]^+$.

Compound 10

BCl_3 (1M solution in dichloromethane) (0.87 mL, 0.87 mmol) was added to a yellow solution of **5** (200mg, 0.22 mmol) in anhydrous dichloromethane (10 mL) in a Schlenk flask resulting in a colour change to dark blue and the reaction mixture was stirred overnight under the dynamic flow of nitrogen. The solvent and excess BCl_3 was removed under reduced pressure. The resulting blue solid was redissolved in anhydrous dichloromethane (10 mL) and then $Zn(C_6F_5)_2$ (193 mg, 0.88 mmol) was added to it. It was then stirred in the closed Schlenk flask overnight at room temperature. Then water 30 mL was added to it and then extracted thrice with dichloromethane. The organic portion was washed with brine and dried over $MgSO_4$. After evaporating the solvent, the residue was purified by column chromatography on base treated (5% Et_3N) silica gel [eluent: 0.5% ethyl acetate in petroleum ether] to afford **10** as a yellow solid. Yield: 215 mg, 91%. ^{1}H NMR (400MHz, $CDCl_3$): δ 8.27 (d, 1H, J = 8 Hz), 8.13 (d, 1H, J = 8 Hz), 8.09 (s, 1H), 8.01-7.98 (m, 2H), 7.91 (d, 1H, J = 8 Hz), 7.84-7.81 (m, 2H), 7.66-7.63 (m, 1H), 7.45-7.39 (m, 7H), 7.36-7.21 (m, 9H), 4.25 (s, 3H), 2.14-2.01 (m, 8H), 1.22-1.12 (m, 48H), 0.84 (t, 12H, J = 6 Hz). ^{13}C NMR (100MHz, $CDCl_3$): 151.4, 151.3, 148.5, 141.9, 141.6, 141.2, 140.5, 137.4, 134.5, 129.2, 128.9, 127.6, 127.5, 127.4, 127.2, 127.1, 126.9, 126.8, 126.4, 125.9, 125.7, 123.0, 122.8, 122.7, 121.2, 120.3, 120.1, 120.0, 115.5, 55.2, 54.6. 46.3, 40.5, 40.3, 31.8, 31.7, 30.1, 30.1, 29.2, 24.0, 23.9, 22.6, 14.1, 14.0, 11.5. ^{11}B NMR (proton decoupled, 128.4 MHz): 2.99 (Broad).HRMS (m/z) calc. for $C_{77}H_{96}BN_3$: 1074.7776, found 1074.7772 $[M+H]^+$.

Compound 11

BCl_3 (1M solution in dichloromethane) (0.87 mL, 0.87 mmol) was added to a yellow solution of **5** (200mg, 0.22 mmol) in anhydrous dichloromethane (10 mL) in a Schlenk flask resulting in a colour change to dark blue and the reaction mixture was stirred overnight under the dynamic flow of nitrogen. The solvent and excess BCl_3 was removed under reduced pressure. The resulting blue solid was redissolved in anhydrous dichloromethane (10 mL) and then $Zn(C_6F_5)_2$ (351 mg, 0.88 mmol) was added to it. It was then stirred in the closed Schlenk flask overnight at room temperature. Then water 30 mL was added to it and then extracted thrice with dichloromethane. The organic portion was washed with brine and dried over $MgSO_4$. After evaporating the solvent, the residue was purified by column chromatography on base treated (5% Et_3N) silica gel [eluent: 0.5% ethyl acetate in petroleum ether] to afford **11** as a yellow solid. Yield: 237mg, 86%. ^{1}H NMR (400MHz, $CDCl_3$):δ8.20 (d, 1H, J = 8 Hz), 7.98-7.96 (m, 1H), 7.93-7.87 (m, 4H), 7.79 (d, 1H, J = 8 Hz), 7.71-7.69 (m, 1H), 7.60-7.58 (m, 1H), 7.33-7.20 (m, 6H), 4.38 (s, 3H), 2.01-1.91 (m, 8H), 1.09-0.98 (m, 48H), 0.70 (t, 12H, J = 4 Hz). ^{13}C NMR (100MHz, $CDCl_3$): 151.5, 151.3, 149.7, 142.7, 142.0, 141.2, 140.7, 140.4, 137.0, 133.9, 130.0, 128.5, 127.6, 127.5, 127.3, 126.9, 127.8, 125.9, 123.5, 123.0, 122.9, 122.8, 122.6, 120.1, 120.1, 120.0, 116.2, 55.3, 54.8, 42.1, 40.4 40.3, 31.8, 31.7, 30.1, 30.0, 29.3, 29.2, 23.9, 22.6, 14.1, 14.0.^{19}F NMR (376.4 MHz, $CDCl_3$): -132.70 (d, J = 22.56 Hz), -157.58 (t, J = 20.68 Hz), -162.52 (t, J = 18.8 Hz). ^{11}B NMR (proton decoupled, 128.4MHz): 1.55 (Broad). HRMS (m/z) calc. for $C_{77}H_{86}BF_{10}N_3$: 1253.6755, found 1253.6775 $[M]^+$.

OLED fabrication

ITO anode structures on glass substrates (size 12 mm × 8 mm) were prepared, which were cleaned for 15 min each in a sequence of ultrasonic baths using acetone, isopropanol, and detergent (Hellmanex III, 2% by volume in DI water). This was followed by oxygen plasma treatment in an Emitech K1050X. Next, a 35 nm thickness film of PEDOT: PSS (Clevios P VP) was deposited as a hole-injecting layer by spin-coating at 3000 rpm for 60 s and annealing in air for 15 min at 135 °C. A 15 nm thick electron-blocking TFB interlayer was then deposited from 2 mg/mL toluene solution by spin coating at 1000 rpm for 30 s and then baking in nitrogen at 180 °C for 1 h. The emissive layer (EML) was deposited on top of the TFB interlayer, again by spin-coating at 2500 rpm for 60 s for the 10 mg/ml PFO: BTz blend solutions (to achieve 60 nm thickness) and spin-coating at 2000 rpm for 60 s for a 10 mg/ml F8BT: BSe blend solution (80 nm thickness). An MBraun thermal evaporator was used to deposit the top cathode comprising calcium (25 nm), and aluminium (100 nm). OLEDs were characterized at room temperature in a sealed sample chamber under nitrogen, using a computer-controlled Keithley source measure unit to apply a bias voltage to the chosen pixel (each substrate accommodated 6 PLED pixels) and to measure the resultant current. For PFO: BTz OLEDs, a Minolta LS100 spot luminance meter measured the corresponding pixel luminance, and EL spectra were recorded using an Ocean Optics USB 2000 CCD spectrometer equipped with a fiber light collection bundle. For F8BT: BSe OLEDs, an Instrument Systems TOP 200 telescopic optical probe connected to a CAS 140CT spectrometer was used to measure the corresponding radiance and EL spectra for each pixel.

Conflicts of interest

There are no conflicts to declare.

Acknowledgements

BD acknowledges funding from the European Union's Horizon 2020 research and innovation programme under the Marie Sklodowska-Curie grant agreement No 660149 (BORCOM). M.J.I. acknowledges the Royal Society (for the award of a University Research Fellowship) and the ERC (Grant Number 305868) and M.L.T. thanks Innovate UK for financial support to the Knowledge Centre for Material Chemistry. The authors acknowledge the UK ESPRC for the Plastic Electronics Centre for Doctoral Training (EP/G037515/1) funding.

Notes and references

1. Z. B. Henson, K. Mullen and G. C. Bazan, *Nat. Chem.*, 2012, **4**, 699.
2. Y. Huang, E. J. Kramer, A. J. Heeger and G. C. Bazan, *Chem. Rev*., 2014, **114**, 7006.
3. A. Creamer, C. S. Wood, P. D. Howes, A. Casey, S. Cong, A. V. Marsh, R. Godin, J. Panidi, T. D. Anthopoulos, C. H. Burgess, T. Wu, Z. Fei, I. Hamilton, M. A. McLachlan, M. M. Stevens and M. Heeney, *Nat. Commun.,* 2018, **9**, 3237.
4. G. C. Welch and G. C. Bazan, *J. Am. Chem. Soc*., 2011, **133**, 4632.
5 For an early example of this approach see: A. Wakamiya, T. Taniguchi, S. Yamaguchi, *Angew. Chem., Int. Ed.,* 2006, **45**, 3170.
6. For reviews on this topic see: (a) F. Jäkle, *Chem. Rev.,* 2010, **110**, 3985. (b) Y-L. Rao and S. Wang, *Inorg. Chem.*, 2011, **50**, 12263. (c) D. Li, H. Zhang, Y. Wang, *Chem. Soc. Rev.*, 2013, **42**, 8416. (d) A. Wakamiya, S. Yamaguchi, *Bull. Chem. Soc. Jpn.*, 2015, **88**, 1357. (e) Main Group Strategies towards Functional Hybrid Materials, Ed. T. Baumgartner and F. Jäkle, 2018, Wiley and Sons.
7. For select examples of N-heterocycle directed C-H electrophilic borylation to form boracycles containing four coordinate boron see: a) N. Ishida, T. Moriya, T. Goya, M. Murakami, *J. Org. Chem*., 2010, **75**, 8709; b) D. L. Crossley, I. A. Cade, E. R. Clark, A. Escande, M. J. Humphries, S. M. King, I. Vitorica-Yrezabal, M. J. Ingleson, M. L. Turner, *Chem. Sci.*, 2015, **6**, 5144 c) D. L. Crossley, J. Cid, L. D. Curless, M. L. Turner and M. J. Ingleson, *Organometallics*, 2015, **34**, 5767. d) A. C. Shaikh, D. S. Ranade, S. Thorat, A. Maity, P. Kulkarni, R. G. Gonnade, P. Munshi, N. T. Patil, *Chem. Commun.*, 2015, **51**, 16115. (e) D. L. Crossley, I. Vitorica-Yrezabal, M. J. Humphries, M. L. Turner and M. J. Ingleson, *Chem. Eur. J.*, 2016, **22**, 12439, (f) M. Yusu, K. Liu, F. Guo, R. A. Lalancette, F. Jäkle *Dalton Trans.*, 2016, **45**, 4580; (g) K. Liu, R. A. Lalancette, F. Jäkle *J. Am. Chem. Soc.*, 2017, **139**, 18170; (h) D. L. Crossley, L. Urbano, R. Neumann, S. Bourke, J. Jones, L. A. Dailey, M. Green, M. J. Humphries, S. M. King, M. L. Turner, M. J. Ingleson *ACS Appl. Mat. Interfaces* 2017, **9**, 28243.
8. C.-P. Chen, Y.-C. Huang, S.-Y. Liou, P.-J. Wu, S.-Y. Kuo and Y.-H. Chan, *ACS Appl. Mat. Interfaces,* 2014, **6**, 21585.
9. C. Saravanan, S. Easwaramoorthi, C.-Y. Hsiow, K. Wang, M. Hayashi and L. Wang, *Org. Lett*., 2014, **16**, 354.
10. R. Yang, R. Tian, Q. Hou, W. Yang and Y. Cao, *Macromolecules*, 2003, **36**, 7453.
11. A. Parthasarathy, S. Goswami, T. S. Corbitt, E. Ji, D. Dascier, D. G. Whitten and K. S. Schanze, *ACS Appl. Mat. Interfaces*, 2013, **5**, 4516.
12. A. Balan, D. Baran, G. Gunbas, A. Durmus, F. Ozyurt and L. Toppare, *Chem. Commun.,* 2009, 6768.
13. A. Balan, G. Gunbas, A. Durmus and L. Toppare, *Chem. Mat.*, 2008, **20**, 7510.
14. H.-M. Shih, R.-C. Wu, P.-I. Shih, C.-L. Wang and C.-S. Hsu, *J. Polym. Sci. A Polym. Chem.,* 2012, **50**, 696.
15. B. J. Lidster, D. R. Kumar, A. M. Spring, C.-Y. Yu and M. L. Turner, *Polym. Chem.,* 2016, 7, 5544.
16. C. M. Cardona, W. Li, A. E. Kaifer, D. Stockdale and G. C. Bazan, *Adv. Mater*., 2011, **23**, 2367.
17. For select examples of comparison of BT vs BSe in D-A materials see: (a) P. Shen, H. Bin, Y. Zhang and Y. Li, *Polym. Chem*., 2014, **5**, 567 (b) E. Zhou, J. Cong, K. Hashimoto, and K. Tajima, *Macromolecules* 2013, **46**, 763.
18. J.-S. Kim, R. H. Friend, I. Grizzi, J. H. Burroughes, *Appl. Phys. Lett.* **2005**, *87*, 023506
19. J. Bailey, E. N. Wright, X. Wang, A. B. Walker, D. D. C. Bradley, J.-S. Kim, *J. Appl. Phys.* **2014**, *115*, 204508.
20. K. Sun, D. Chu, Y. Cui, W. Tian, Y. Sun and W. Jiang, *Org. Electron.*, 2017, **48**, 389-396.
21. S. Tang, P. Murto, X. Xu, C. Larsen, E. Wang and L. Edman, *Chem. Mater.*, 2017, **29**, 7750-7759.